

Tumor-Selective Response to Antibody-Mediated Targeting of $\alpha_v\beta_3$ Integrin in Ovarian Cancer¹

Charles N. Landen^{*}, Tae-Jin Kim[†], Yvonne G. Lin^{*}, William M. Merritt^{*}, Aparna A. Kamat^{*}, Liz Y. Han^{*}, Whitney A. Spannuth^{*}, Alpa M. Nick^{*}, Nicholas B. Jennings^{*}, Michael S. Kinch[‡], David Tice[§] and Anil K. Sood^{*,†}

^{*}Department of Gynecologic Oncology, The University of Texas M.D. Anderson Cancer Center, 1155 Herman Pressler Boulevard, Unit 1362, Houston, TX 77030, USA; [†]Division of Gynecologic Oncology, Department of Obstetrics and Gynecology, Cheil General Hospital, Kwandong University College of Medicine, Seoul, South Korea; [‡]Functional Genetics, 708 Quince Orchard Rd, Gaithersburg, MD 20878, USA; [§]MedImmune, Inc., 1 MedImmune Way, Gaithersburg, MD 20878, USA; [¶]Department of Cancer Biology, The University of Texas M.D. Anderson Cancer Center, 1515 Holcombe Boulevard, Unit 173, Houston, TX 77030, USA

Abstract

The $\alpha_v\beta_3$ integrin is expressed on proliferating endothelial cells and some cancer cells, but its expression on ovarian cancer cells and its potential as a therapeutic target are unknown. In this study, expression of the $\alpha_v\beta_3$ integrin on ovarian cancer cell lines and murine endothelial cells was tested, and the effect of a fully humanized monoclonal antibody against $\alpha_v\beta_3$, Abegrin (etaracizumab), on cell invasion, viability, tumor growth, and the Akt pathway were examined *in vitro* and *in vivo*. We found that etaracizumab recognizes $\alpha_v\beta_3$ on the ovarian cancer cell lines SKOV3ip1, HeyA8, and A2780ip2 (at low levels) but not on *murine* endothelial cells. Etaracizumab treatment decreased ovarian cancer proliferation and invasion. *In vivo*, tumor-bearing mice treated with etaracizumab alone gave variable results. There was no effect on A2780ip2 growth, but a 36% to 49% tumor weight reduction in the SKOV3ip1 and HeyA8 models was found ($P < .05$). However, combined etaracizumab and paclitaxel was superior to paclitaxel in the SKOV3ip1 and A2780ip2 models (by 51-73%, $P < .001$) but not in the HeyA8 model. Treatment with etaracizumab was then noted to decrease p-Akt and p-mTOR in SKOV3ip1, but not in HeyA8, which is Akt-independent. Tumors resected after therapy showed that etaracizumab treatment reduced the proliferating cell nuclear antigen index but not microvessel density. This study identifies tumor cell $\alpha_v\beta_3$ integrin as an attractive target and defines the Akt pathway as a predictor of response to function-blocking antibody.

Neoplasia (2008) 10, 1259–1267

Abbreviations: ECM, extracellular matrix; MICS, Membrane Invasion Culture System; IP, intraperitoneal; eta, etaracizumab

Address all correspondence to: Anil K. Sood, MD, Professor, Departments of Gynecologic Oncology and Cancer Biology, The University of Texas M.D. Anderson Cancer Center, 1155 Herman Pressler, CPB6.3244, Unit 1362, Houston, TX 77230-1439. E-mail: asood@mdanderson.org

¹Funding: In part by the Reproductive Scientist Development Program through the Ovarian Cancer Research Fund and the National Institutes of Health (K12 HD00849, to C.N.L.); the Department of Defense (W81XWH-04-1-0227); the University of Texas MD Anderson Cancer Center Specialized Program of Research Excellence in ovarian cancer (CA083639); National Institutes of Health grants CA10929801 and CA11079301; Program Project Development Grant from the Ovarian Cancer Research Fund, Inc.; and the Marcus Foundation (to A.K.S.).

Received 3 July 2008; Revised 14 August 2008; Accepted 19 August 2008

Copyright © 2008 Neoplasia Press, Inc. All rights reserved 1522-8002/08/\$25.00
DOI 10.1593/neo.08740

Introduction

Integrins are a family of cell surface receptors that are primarily responsible for exchanging information between cells and the surrounding extracellular matrix (ECM) [1]. They are heterodimers composed of 1 of 10 α subunits and 1 of 8 β subunits, and each subtype has specificity for different ECM proteins. In response to binding components of the ECM, such as collagen, fibronectin, or vitronectin, signals are generated within the cell that can affect growth, migration, invasion differentiation, and survival [2,3]. As more is learned about the importance of a tumor cell's microenvironment to survival and invasive potential, integrins are seen to play an important role in tumor biology and may serve as useful targets to tumor therapy.

The $\alpha_v\beta_3$ integrin [4] is preferentially expressed on developing, rather than mature vasculature, and is considered the most important integrin for angiogenesis [5]. Its primary ligand is vitronectin, but it also interacts with fibrinogen, fibronectin, and thrombospondin [6,7]. Furthermore, associations have been found between $\alpha_v\beta_3$ and matrix metalloproteinase 2, platelet-derived growth factor, insulin, and vascular endothelial growth factor receptor 2 (VEGFR-2) [8–11]. In a self-promoting loop, VEGF, one of the more potent stimulators of angiogenesis [12,13], up-regulates $\alpha_v\beta_3$ expression and increases affinity for its ligands [14], which in turn interacts with VEGFR-2 to further amplify VEGF [15]. Administration of a mouse monoclonal antibody against $\alpha_v\beta_3$ (LM609) was shown to disrupt tumor-induced angiogenesis on chick chorioallantoic membrane (CAM) [5], and in subsequent studies, disrupt tumor-associated vasculature and induce tumor regression without significant adverse effects on established, mature blood vessels. Subsequent studies of the LM609 antibody showed tumor growth inhibition in preclinical mouse models of melanoma [16,17] and breast cancer [18], and synergy with immunotherapy in neuroblastoma [19].

More recently, $\alpha_v\beta_3$ expression has been demonstrated on metastatic human melanoma, breast, prostate, and glioblastoma tumor cells, where its expression contributes to malignant phenotype. A fully humanized antibody targeted to $\alpha_v\beta_3$ has demonstrated encouraging activity (etaracizumab, Abegrin; MedImmune, Inc., Gaithersburg, MD) [20]. The $\alpha_v\beta_3$ integrin has been studied in ovarian cancer, with targeting by either antibodies or small molecule inhibitors shown to inhibit migration, adhesion, motility, angiogenesis, and proliferation *in vitro* [11,21–24]. The α_v subunit has been found in malignant effusions and solid tumors from ovarian cancer patients [25]. However, the biologic significance of $\alpha_v\beta_3$ targeting is not fully understood. The aim of this study was to determine the effects of $\alpha_v\beta_3$ on ovarian cancer cell line invasion, proliferation, vascularization, and tumor growth in an *in vivo* orthotopic model of advanced ovarian cancer. Examining several cell lines *in vivo*, we have also identified molecular correlates of anti- $\alpha_v\beta_3$ therapy. These findings support the use of etaracizumab as therapy for ovarian cancer and demonstrate the benefit of tailoring therapy based on an individual's tumor biology.

Materials and Methods

Cell Lines and Culture

The ovarian cancer cell lines HeyA8, SKOV3ip1, A2780, and A2780ip2 [26,27] were maintained in RPMI 1640 supplemented with 15% FBS and 0.1% gentamicin sulfate (Gemini Bioproducts, Calabasas, CA). The A2780ip2 line was developed by culture of tu-

mors grown in the mouse intraperitoneal (IP) cavity after IP injection of A2780, through two passes. Endothelial cells isolated from the mesentery or ovary of the immortomouse were a kind gift from Dr. Robert Langley [28] and maintained in DMEM with 10% FBS. These cells proliferate indefinitely by means of SV40 transformation at 33°C. However, when switched to 37°C, SV40 expression is turned off, and cells proliferate for only a few more cycles [28]. When using these cells, they were kept at 37°C for 48 hours before any experiments were performed, to allow elimination of SV40 expression. All *in vitro* experiments were conducted at 60% to 80% confluence, unless otherwise specified. For vitronectin-coating experiments, 20 $\mu\text{g/ml}$ vitronectin (Chemicon, Temecula, CA) in PBS (or PBS alone) was added to culture vessels and incubated at 37°C overnight. Afterwards, vitronectin/PBS was removed and replaced with 1% bovine serum albumin in PBS for 1 hour at 37°C. This was then removed immediately before plating cells for an experiment. For *in vivo* injection, cells were trypsinized and centrifuged at 1000 rpm for 7 minutes at 4°C, washed twice, and reconstituted in Hank's balanced salt solution (Gibco, Carlsbad, CA) at a concentration of 5×10^6 cells/ml for 200- μl IP injections of 1×10^6 cells.

Flow Cytometry

Cells growing in monolayer culture at 60% to 80% confluence were trypsinized with EDTA and washed in PBS. Cells were reconstituted to equal 5×10^6 cell/ml, and 200 μl was incubated with 1 $\mu\text{g/ml}$ anti- $\alpha_v\beta_3$ antibody (LM609; Upstate, San Francisco, CA) with gentle rotation at 4°C for 30 minutes. Cells were spun at 2000 rpm for 5 minutes, washed twice with PBS, and reincubated with antimouse IgG-FITC (Upstate) at 4°C for 30 minutes. Cells were washed with PBS and reconstituted in 1 ml of PBS for immediate reading with an EPICS XL-MCL flow cytometer (Beckman Coulter Inc., Miami, FL).

Immunoprecipitation and Western Blot

Immunoblot detection of α_v and β_3 integrin subunits was performed using a modified immunoprecipitation technique that not only allowed detection of both α_v and β_3 together in a single sample but also allowed detection of other integrin subunits associated with either α_v or β_3 . Cells in monolayer culture were labeled with biotin, and cell lysates were prepared by washing cells with PBS followed by incubation in modified RIPA lysis buffer (50 mM Tris, 150 mM NaCl, 1% Triton, 0.5% deoxycholate plus 25 $\mu\text{g/ml}$ leupeptin, 10 $\mu\text{g/ml}$ aprotinin, 2 mM EDTA, and 1 mM sodium orthovanadate; Sigma Chemical Co., St. Louis, MO) for 10 minutes at 4°C. Cells were scraped from plates and centrifuged at 13,000 rpm for 20 minutes at 4°C, and the supernatant was stored at -80°C. Protein concentrations were determined using a BCA Protein Assay Reagent kit (Pierce Biotechnology, Rockford, IL), and samples were separated for α_v or β_3 testing. Protein (300 μg) was immunoprecipitated with either anti- α_v antibody (Chemicon, Temecula, CA), anti- β_3 antibody (Cell Signaling), or control IgG antibody in PBS for 30 minutes at 4°C, followed by protein A sepharose beads 50% slurry for 30 minutes at 4°C. Protein was eluted from beads in reducing Laemmli buffer, and were beads separated from the lysate by centrifugation. Samples were subjected to 10% SDS-PAGE separation and transferred to a nitrocellulose membrane by semidry electrophoresis (Bio-Rad Laboratories, Hercules, CA), and biotin was detected with 1.0 $\mu\text{g/ml}$ HRP-conjugated antimouse IgG (Amersham, Piscataway, NJ), and developed using enhanced chemiluminescence detection kit (ECL; Pierce).

For immunoblot detection of other proteins, cells were collected in modified RIPA lysis buffer as above (without prior incubation with biotin). After BCA quantification, 50 μg of protein lysate in Laemmli buffer was subjected to 10% SDS-PAGE separation and transferred to a nitrocellulose membrane. After blocking the membrane with 5% milk in TBS-0.1% Tween 20 (TBS-T), they were incubated with the appropriate primary antibody overnight at 4°C (anti-phosphorylated Akt, anti-total Akt2, anti-total Akt1, anti-phosphorylated PI3K, and anti-phosphorylated mTOR from Cell Signaling; and anti- β -actin from Sigma). After washing with TBS-T, appropriate secondary antibody was applied (anti-mouse IgG-HRP and anti-rabbit IgG-HRP from Amersham) for 1 hour at room temperature; the membrane was washed with TBS-T and developed with ECL as above.

Cell Invasion

Invasion through a human-defined matrix was assessed using the Membrane Invasion Culture System (MICS). Briefly, this system consists of an upper chamber loaded with cells and a lower chamber with fibroblast-derived chemoattractants into which cells may invade, through a semiporous membrane coated with laminin, collagen, vitronectin, and fibronectin. A total of 100,000 cells in media containing control human IgG (10 $\mu\text{g}/\text{ml}$) or etaracizumab (1 or 10 $\mu\text{g}/\text{ml}$) were loaded into the upper chamber and allowed to invade for 24 hours. The cells migrating into the lower chamber were collected, fixed onto a membrane, stained, and counted by microscopy by an examiner blinded to the experimental group.

Cell Viability Assay

To determine effects on cell proliferation and sensitivity to docetaxel, 2000 cells were plated in each well of a 96-well plate, and experimental conditions were set in triplicate 24 hours after cell plating. Before plating cells, plates were either uncoated or coated with vitronectin (the primary $\alpha_v\beta_3$ ligand) by incubating plates in 50 μl of 10 $\mu\text{g}/\text{ml}$ vitronectin (Chemicon) for 2 hours at room temperature, followed by the removal of vitronectin solution and storage at 4°C for 12 hours. To assess viability after etaracizumab treatment, cells were incubated with 200 μl of serum-containing growth media containing increasing concentrations of etaracizumab. For docetaxel sensitivity experiments, cells were exposed to increasing concentrations of docetaxel with 25 $\mu\text{g}/\text{ml}$ etaracizumab (one-time treatment) or 25 $\mu\text{g}/\text{ml}$ of non-specific human IgG (Jackson Laboratory, Bar Harbor, ME). Cell viability was assessed by MTT assay after 5 to 7 days, at which time 50 μl of 0.15% MTT (Sigma) was added to each well. After incubation for 2 hours at 37°C, the media/MTT was removed, and cells were reconstituted in 100 μl of DMSO (Sigma). After shaking, the absorbance at 570 nm was recorded using a FALCON microplate reader (Becton Dickinson Labware, Franklin Lakes, NJ). The IC_{50} was determined by calculating the mean OD_{570} ($[\text{Max OD} - \text{Min OD}] / 2 + \text{Min OD}$) and finding the docetaxel concentration at which this OD reading intersected the dose-response curve.

Orthotopic In Vivo Model and Tissue Processing

Female athymic nude mice (NCr-*nu*) were purchased from the National Cancer Institute – Frederick Cancer Research and Development Center (Frederick, MD) and housed in specific pathogen-free conditions. They were cared for in accordance with guidelines set forth by the American Association for Accreditation of Laboratory Animal Care and the U.S. Public Health Service *Policy on Human*

Care and Use of Laboratory Animals, and all studies were approved and supervised by the UT MD Anderson Cancer Center Institutional Animal Care and Use Committee. For long-term experiments to assess tumor growth, therapy began 1 week after IP cell injection of 1×10^6 cells (see the Cell Lines and Culture section). Therapy consisted of four groups: 1) Control human IgG, 2) etaracizumab, 3) paclitaxel plus control IgG, or 4) paclitaxel plus etaracizumab. Antibodies were diluted in PBS and injected intraperitoneally twice per week, at a dose of 10 mg/kg, in a volume of 180 to 220 μl (depending on mouse weight). Paclitaxel was diluted in PBS and injected IP once a week, at a dose of 100 μg , in 200 μl . Mice were monitored for adverse effects, and the experiment concluded if animals in any group began to appear moribund and required sacrifice or if any tumor-bearing animal was found dead from tumor burden (generally 4-5 weeks after cell injection). All animals in the experiment were killed together by cervical dislocation. Mouse weight, tumor weight, and distribution of tumor were recorded by examiners blinded to experimental group. Tissue specimens were snap frozen for lysate preparation, fixed in formalin for paraffin embedding, and frozen in OCT media for frozen slide preparation.

Immunohistochemistry

Staining for proliferating cell nuclear antigen (PCNA) and CD31 was conducted on tumors collected at the conclusion of 4-week therapy trials. Formalin-fixed, paraffin-embedded sections were deparaffinized by sequential washing with xylene, 100% ethanol, 95% ethanol, 80% ethanol, and PBS. After antigen retrieval (described below), endogenous peroxidase was blocked with 3% H_2O_2 in methanol for 5 minutes. After washing twice in PBS, slides were blocked with 5% normal horse serum and 1% normal goat serum in PBS for 15 minutes at room temperature, followed by incubation with primary antibody in blocking solution overnight at 4°C. After washing twice with PBS, the appropriate secondary antibody conjugated to horseradish peroxidase, in blocking solution, was added for 1 hour at room temperature. HRP was detected with DAB (Phoenix Biotechnologies, Huntsville, AL) substrate for 5 minutes, washed, and counterstained with Gil No. 3 hematoxylin (Sigma) for 20 seconds. Primary antibodies used included anti-CD31 (PECAM-1, rat IgG; Pharmingen, San Jose, CA) and anti-PCNA (PC-10, mouse IgG; Dako, Carpinteria, CA). Immunohistochemistry for PCNA was performed on paraffin-embedded slides with antigen retrieval of microwave heating for 5 minutes in 0.1 M citrate buffer, pH 6.0. Immunohistochemistry for CD31 was performed on freshly cut tissue frozen in OCT. These slides were fixed in cold acetone for 10 minutes and did not require antigen retrieval.

Statistics

Continuous variables were compared with the Student's *t* test (between two groups) or analysis of variance (for all groups) if normally distributed and the Mann-Whitney rank sum test if nonparametric. For *in vivo* therapy experiments, 10 mice in each group were used, as directed by a power analysis to detect a 50% reduction in tumor size (β error = 0.2). A $P < .05$ on 2-tailed testing was considered significant.

Results

The $\alpha_v\beta_3$ Integrin Is Expressed by Ovarian Cancer Cells

Although the $\alpha_v\beta_3$ integrin was initially thought to primarily be expressed by proliferating and immature endothelial cells, it has also

been found on some tumor cells [29–32]. To determine whether ovarian cancer cell lines express $\alpha_v\beta_3$, we performed flow cytometry (Figure 1A) and Western Blot (Figure 1B) analyses to detect protein expression. The SKOV3ip1 and HeyA8 cell lines have prominent $\alpha_v\beta_3$ recognition by the LM609 primary antibody, the murine antibody from which the fully humanized etaracizumab was derived and shares the Fab' construct. The A2780ip2 cell line has less prominent expression, but a definite population with $\alpha_v\beta_3$ expression (estimated at 9.8% of cells, experiment repeated twice with identical results). Furthermore, β_3 expression was seen in A2780 lysate from tumor samples collected at the conclusion of *in vivo* studies described below, suggesting $\alpha_v\beta_3$ expression is up-regulated *in vivo* compared to *in vitro* (data not shown). After immunoprecipitation with α_v , β_3 , or control IgG, presence of the α_v subunit was prominent in all three cell lines, and β_3 expression was high in SKOV3ip1 and HeyA8 but low in A2780. The presence of additional bands (compared with IgG) with α_v but not with β_3 indicates that the α_v subunit forms heterodimers with β subunits other than β_3 (though less commonly), but the only α subunit that β_3 forms a heterodimer with is α_v . The etaracizumab antibody does not interact with other integrins, including $\alpha_v\beta_5$ (data not shown). Importantly, the antibody also does not recognize murine $\alpha_v\beta_3$, as reported previously [33] and

confirmed by FACS analysis of cultured murine endothelial cells (Figure 1A).

Etaracizumab Inhibits *In Vivo* Tumor Growth in an Orthotopic Mouse Model of Ovarian Cancer

We next examined whether treatment with etaracizumab could reduce tumor growth in an *in vivo* orthotopic mouse model of advanced ovarian cancer in all three cell lines (SKOV3ip1, A2780ip2, and HeyA8). After IP cell injection, mice were randomized to four treatment groups ($n = 10$ mice per group): 1) control human IgG, 10 mg/kg twice per week; 2) etaracizumab, 10 mg/kg twice per week; 3) paclitaxel, 100 μ g weekly plus control IgG; or 4) paclitaxel plus etaracizumab (given at doses listed above). All treatments were administered intraperitoneally. Animals were treated until mice in any group became moribund, at which point all mice in an experiment were killed (4–5 weeks). In the SKOV3ip1 model (Figure 2A), etaracizumab alone reduced tumor growth by 48.8% compared to IgG ($P = .041$). Paclitaxel, as previously seen in this model, reduced growth by 66% ($P < .01$ vs IgG and $P = .06$ vs etaracizumab). The combination of paclitaxel and etaracizumab significantly reduced growth by 83.3% compared to control IgG alone ($P < .001$) and by 50.8% compared to paclitaxel/IgG ($P = .01$). Etaracizumab alone, paclitaxel alone, and

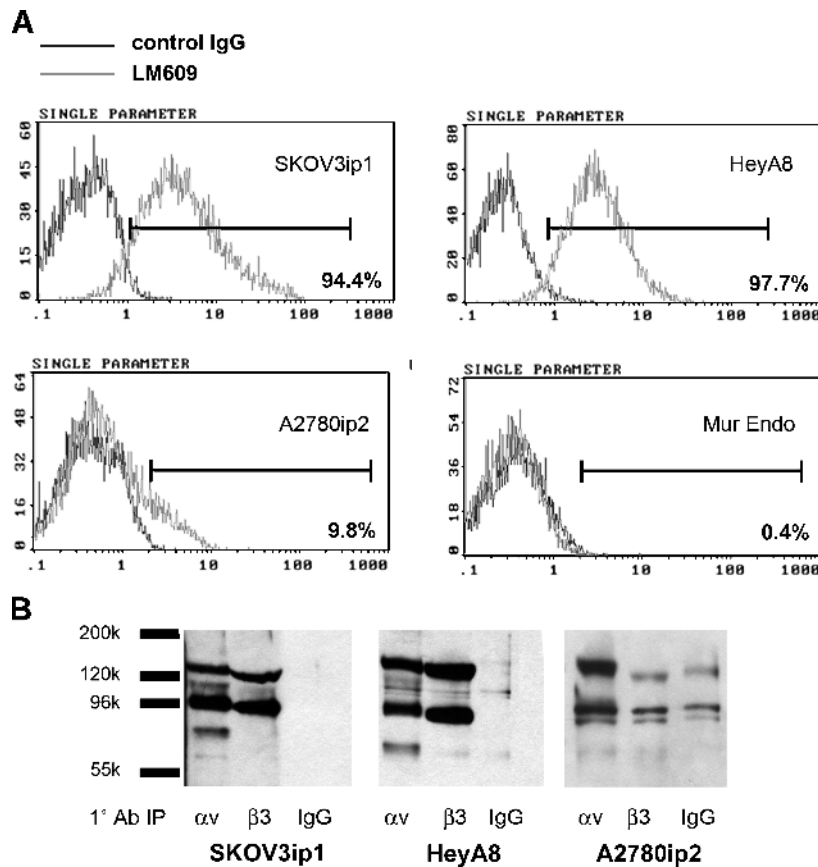


Figure 1. Expression of $\alpha_v\beta_3$ in ovarian cancer cell lines. Recognition of the $\alpha_v\beta_3$ heterodimer was assessed first by flow cytometry, using the murine monoclonal antibody clone LM609 as primary antibody (A). This is the clone from which the etaracizumab antibody was derived and shares identical Fab' regions. There is a high expression of $\alpha_v\beta_3$ in the SKOV3ip1 and HeyA8 lines, and expression in a smaller population in A2780ip2. LM609 does not bind to $\alpha_v\beta_3$ in murine endothelial cells. Modified immunoprecipitation was then performed, where cells were exposed to biotin in culture, immunoprecipitated with anti- α_v , anti- β_3 , or control IgG, then separated by SDS-PAGE electrophoresis (B). Bands at the expected location of the α_v and β_3 integrin subunits (125 and 105 kDa, respectively) are noted when either primary antibody was used in SKOV3ip1 and HeyA8. Expression in A2780ip2 was not high enough to be detected by this method.

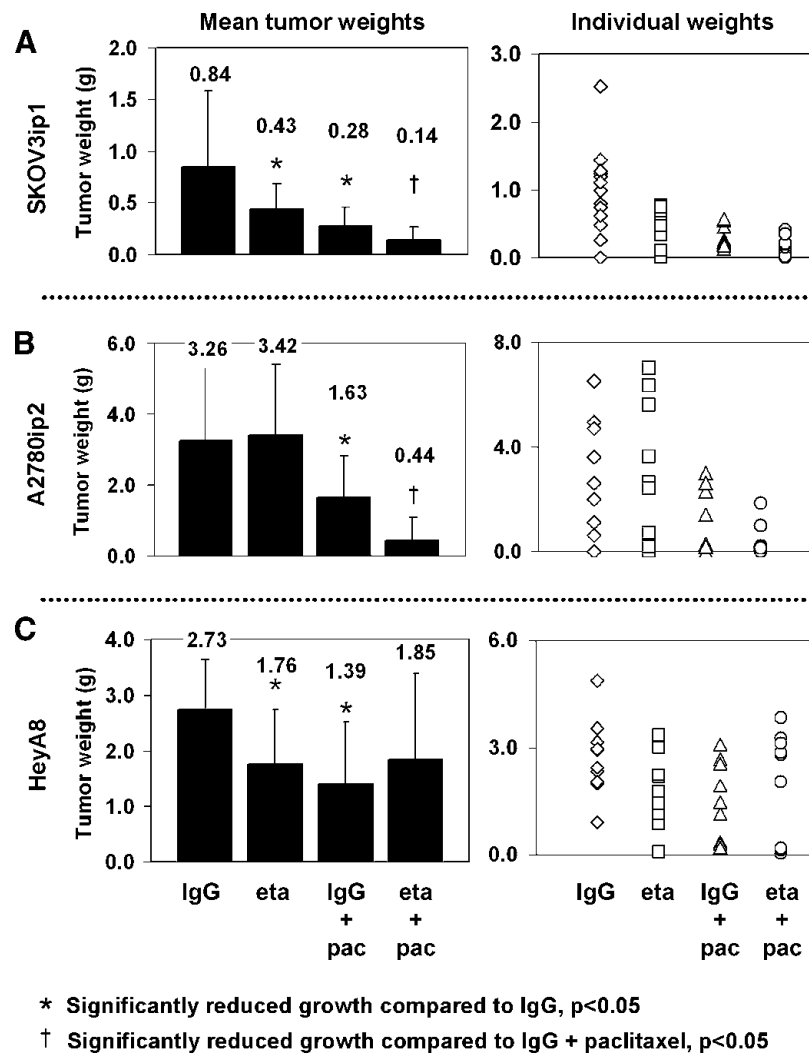


Figure 2. Effect of therapy on tumor growth. Nude mice were injected intraperitoneally with SKOV3ip1 (A), A2780ip2 (B), or HeyA8 (C) cells. One week after injection, therapy began with control IgG, etaracizumab (eta), paclitaxel (Pac) plus IgG, or etaracizumab plus paclitaxel. Antibodies were given twice weekly at a dose of 10 mg/kg, paclitaxel once weekly at a dose of 100 μ g, all administered intraperitoneally. All animals in an experiment were killed when control animals became moribund from tumor, and total tumor weight was measured. Mean weights \pm SD are shown on the left; individual tumor measurements are shown on the right. Weights between the two groups were compared with the Student's *t* test if values were normally distributed and the Mann-Whitney rank sum test if non-parametric. Etaracizumab alone was superior to IgG in SKOV3ip1 and HeyA8, the two lines with highest $\alpha_v\beta_3$ expression. Addition of etaracizumab to paclitaxel was superior to paclitaxel with IgG in the SKOV3ip1 and A2780ip2 models.

the combination were all effective in reducing the number of nodules formed and preventing ascites formation, though combination therapy was not significantly different compared to either single-agent therapy in these parameters (data not shown).

In the A2780ip2 model (Figure 2B), different effects of therapy were noted. Tumor weight after etaracizumab treatment was not significantly different from that of IgG-treated tumors. However, when combined with paclitaxel, treatment significantly reduced tumor growth by 86.4% compared to control mice ($P = .029$) and by 72.8% compared to paclitaxel/IgG ($P = .14$). The striking difference between response to etaracizumab with and without paclitaxel suggests some mechanism of additional benefit with the combination in this model.

In the HeyA8 model, a different response pattern was seen (Figure 2C). In this model, etaracizumab therapy alone did significantly reduced tumor weight, by 35.6% ($P = .047$). However, tumors sub-

jected to combination therapy with etaracizumab and paclitaxel had comparable weights to etaracizumab alone, that is, 32.3% larger tumors than paclitaxel/IgG ($P = .46$). These responses suggest that biologic processes allowing additional benefit in the other models is absent in the HeyA8 model.

Response to Combination Therapy Can Be Explained by Dependence on the Akt Pathway

A positive response seen with etaracizumab alone in the SKOV3ip1 and HeyA8 cell lines, but not in A2780ip2 was not surprising, given the low expression of $\alpha_v\beta_3$ in A2780ip2. However, an explanation for the positive response to chemotherapy in this line and SKOV3ip1, but not HeyA8, was not readily apparent. The HeyA8 cell line contains a *BRAF* mutation and, therefore, is primarily dependent on the Ras/Raf/Erk pathway for its proliferative capacity [34]. The SKOV3ip1 line, conversely, has constitutive activation of Akt, as does

the A2780ip2 line, which contains a *PTEN* mutation [35]. Because of these differences in biology, we examined the effect of etaracizumab treatment on members of the Akt pathway in SKOV3ip1 and HeyA8. Cells were incubated with etaracizumab or control IgG in 0.5% FBS media for 15 minutes, then plated onto vitronectin-coated plates. After 24 hours, cells were harvested as lysate and subjected to Western blot analysis of phospho-Akt (Figure 3). Although etaracizumab decreased the degree of p-Akt by 39% in the SKOV3ip1 cells, it did not affect the barely detectable p-Akt in HeyA8. After membrane stripping and reprobing for total Akt2 (the predominant Akt isoform in ovarian can-

cer), followed by total Akt1, treatment with etaracizumab actually led to a decrease in total Akt of both isoforms (36% and 45% reductions, respectively). Interestingly, etaracizumab led to activation of the 55-kDa subunit of PI3K, which may be a compensatory response to decreasing total Akt. Finally, a decrease in Akt phosphorylation was associated with a decrease in phosphorylated mTOR, a prominent downstream effector of the Akt pathway. Because the p-Akt signal in HeyA8 at 24 hours was barely detectable, we repeated the experiment to collect cells after 5 minutes of vitronectin exposure (20 total minutes of etaracizumab exposure) in serum-free media. This condition led to activation of Akt, which was not prevented by etaracizumab. This also confirms that although Akt is not constitutively activated in HeyA8, it is capable of being phosphorylated. This profile persisted at 30 minutes, but Akt was back to near undetectable levels after 4 hours (data not shown). The mTOR protein is not activated to a significant degree in HeyA8.

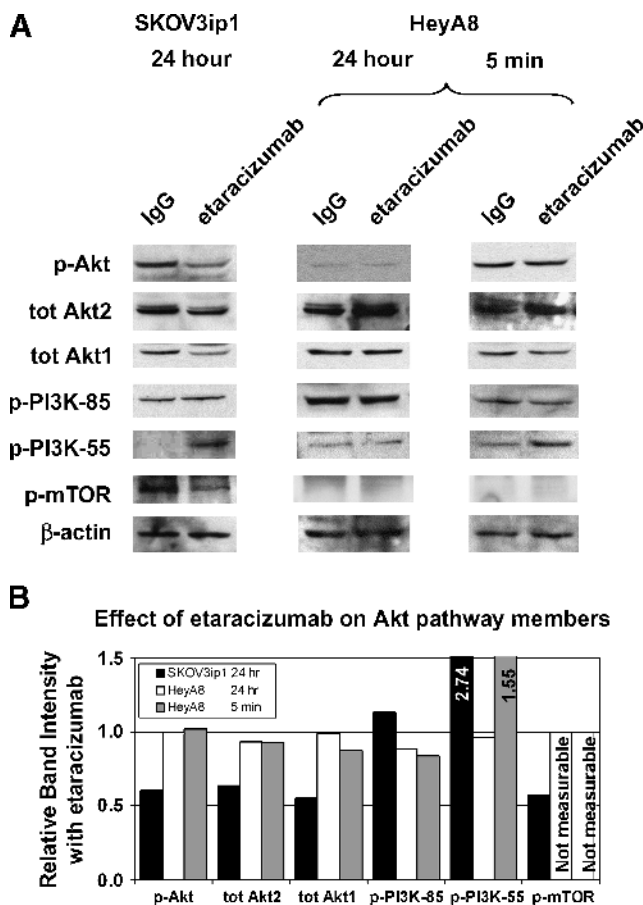


Figure 3. Effects of etaracizumab on the AKT pathway. To explore an explanation for the differential effects seen *in vivo* in SKOV3ip1 and HeyA8 despite $\alpha_v\beta_3$ expression, we examined effects of exposure to etaracizumab on cells plated on vitronectin. Cell lysate from cells exposed for 24 hours was collected and tested for phosphorylated Akt (p-Akt), total Akt2 (tot Akt2), total Akt1 (tot Akt1), phosphorylated PI3 kinase 85-kDa subunit (p-PI3K-85), phosphorylated PI3 kinase 55-kDa subunit (p-PI3K-55), phosphorylated mTOR (p-mTOR), and β -actin (A). Band intensity was quantified with Scion Image and normalized with β -actin band intensity, and the change noted with etaracizumab is shown (B). At 24 hours in the SKOV3ip1 cell line, phosphorylated Akt, total Akt1, and total Akt2 were all decreased with treatment, as was phosphorylated mTOR. Interestingly, phosphorylated PI3K–55-kDa subunit was increased with treatment. No treatment effect was seen in HeyA8 at 24 hours, although the pathway was shown to be intact by higher phosphorylated Akt (in both treatment groups) at 5 minutes, likely a transient effect due to a change to low-serum media. Phosphorylated mTOR was not measurable (NM) in HeyA8 at 5 minutes and 24 hours.

Mechanisms of Etaracizumab Effects: Analysis of Proliferation, Invasion, and Angiogenesis

On the basis of the observed *in vivo* effects, we next asked whether etaracizumab could directly inhibit tumor cell proliferation. *In vitro*, cells were first plated on uncoated 96-well culture plates with increasing doses of etaracizumab and allowed to proliferate for 5 days, and cell viability was measured by the MTT assay. Etaracizumab did not affect proliferation under these conditions (Figure 4A, open bars). Subsequently, the effects of etaracizumab were examined after coating the tissue culture plates with vitronectin, the primary matrix for $\alpha_v\beta_3$. At low doses, vitronectin potentiated cell growth (Figure 4A, closed bars). However, with treatment of etaracizumab, growth is significantly inhibited in a dose-dependent fashion. These data indicate that blocking $\alpha_v\beta_3$ has a negative effect on *in vitro* cell proliferation only if its matrix receptor is present. In docetaxel sensitivity experiments with concurrent treatment with etaracizumab and increasing doses of docetaxel, etaracizumab did not sensitize SKOV3ip1 or A2780ip2 cells to docetaxel (data not shown). This suggests that paclitaxel-sensitizing effects of etaracizumab in the SKOV3ip1 and A2780ip2 models are dependent on the correct *in vivo* microenvironment.

To analyze proliferation *in vivo*, representative tumors collected at the conclusion of therapy experiments were stained for PCNA. The percentage of PCNA-positive cells was calculated and shown in Figure 4B. Etaracizumab, paclitaxel, and combination therapy were all found to reduce the percentage of proliferating cells by 31% to 45% compared to control IgG-treated samples ($P < .05$). Combination therapy was not significantly different from either single-agent treatment, despite the finding that SKOV3ip1 and A2780ip2 tumors were smaller with combination therapy.

Because inhibition of $\alpha_v\beta_3$ integrin can have antiangiogenic effects by targeting endothelial cells, tumors were then evaluated for microvessel density by staining with CD31. The mean number of vessels per high-powered field was calculated, and no significant difference between groups was seen (Figure 4C). This was not an unexpected finding, given the lack of recognition of murine $\alpha_v\beta_3$ integrin that would be expressed by the host endothelial cells.

On the basis of the potential role of the $\alpha_v\beta_3$ integrin in cell movement, we next examined the effects of etaracizumab on ovarian cancer cell invasion using the MICS. In the presence of increasing doses of etaracizumab (1 or 10 $\mu\text{g/ml}$ vs 10 $\mu\text{g/ml}$ control human IgG), the percent of cells invading through the membrane were compared. In a dose-dependent manner, etaracizumab significantly inhibited

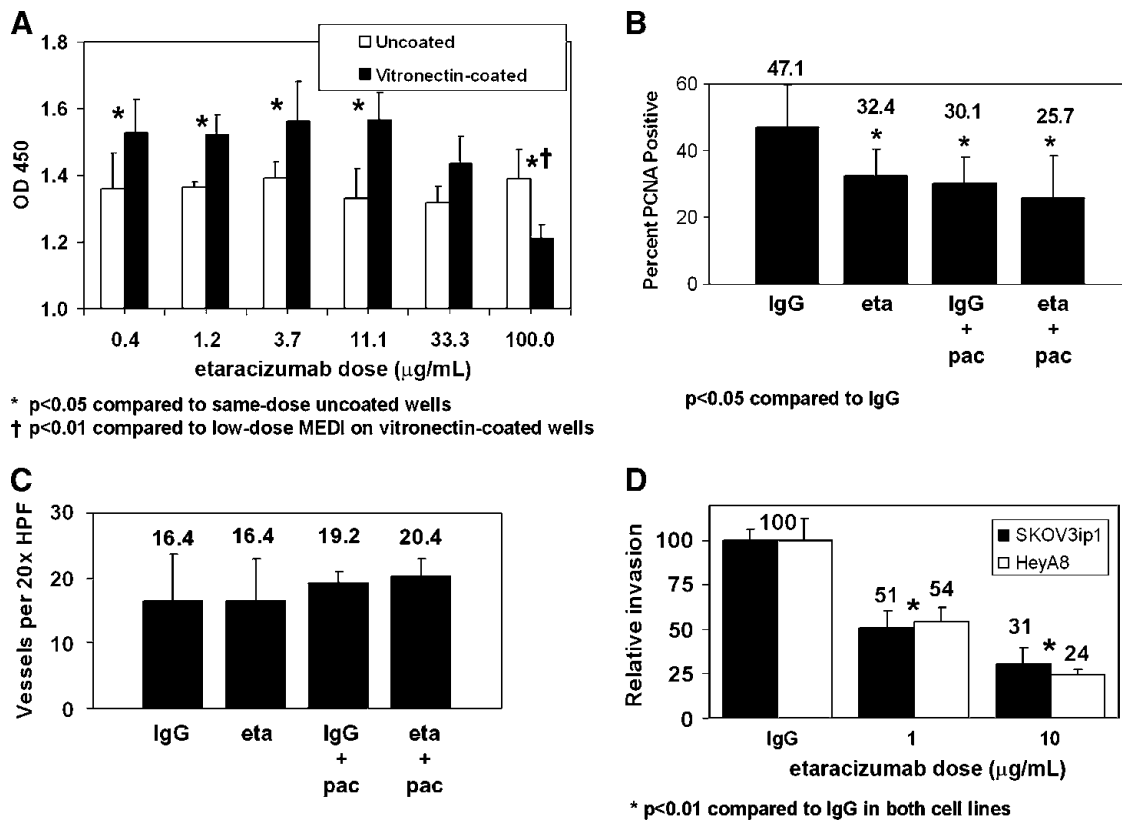


Figure 4. Mechanisms of etaracizumab effects on ovarian cancer. In an MTT viability assay, cells were allowed to grow on uncoated wells or wells precoated with vitronectin, with increasing concentrations of etaracizumab (A). At low concentrations of etaracizumab, vitronectin promoted cell viability. However, at higher concentrations of etaracizumab, viability was inhibited on cells grown on vitronectin, the $\alpha_v\beta_3$ receptor. Etaracizumab did not affect viability when wells were not precoated with vitronectin. Data shown is in SKOV3ip1, with HeyA8 giving similar results. To assess *in vivo* effects on tumor biology, tumors were collected at the conclusion of the therapy experiments described in Figure 2 and tested for proliferation index as determined by PCNA positivity (B) and microvessel density as determined by number of CD31-positive lumens (C). The mean number of PCNA-positive cells or vessels in five randomly selected fields were counted and compared between groups. Consistent with *in vitro* proliferation data, etaracizumab (eta) reduced the proliferation index compared to IgG-exposed tumors, though there was no significant difference between IgG/paclitaxel- (IgG + pac) and etaracizumab/paclitaxel- (eta + pac) treated tumors. However, all four groups were similar in microvessel density, which may be a reflection of the lack of recognition of the murine $\alpha_v\beta_3$ integrin by etaracizumab. Finally, using the MICS, cell invasion through a human defined matrix in SKOV3ip1 and HeyA8 were examined with and without etaracizumab (D). Blockade of $\alpha_v\beta_3$ leads to a dose-dependent inhibition of invasion in both cell lines.

invasion (Figure 4D). Collectively, these findings indicate a direct inhibitory effect of etaracizumab on ovarian cancer cell proliferation and invasion. No appreciable difference in microvessel density may be primarily due to a lack of recognition of murine $\alpha_v\beta_3$ integrin on tumor endothelial cells by etaracizumab.

Discussion

We have demonstrated that $\alpha_v\beta_3$ is expressed on ovarian cancer cell lines and that blocking this integrin with etaracizumab results in reduced proliferation *in vitro* and *in vivo*, reduced invasion, and inhibition of tumor growth when used in combination with paclitaxel. The response to therapy could be predicted by the expression of $\alpha_v\beta_3$ and dependence on the AKT pathway for each cell line (Table 1). These data are the first demonstrating *in vivo* efficacy in an ovarian cancer model, and offer encouraging evidence that etaracizumab may be effective in treating ovarian cancer in a clinical setting. Of note, because the antibody used does not cross-react with murine $\alpha_v\beta_3$, these responses represent direct effects on tumor cells. It is possible

that additional antivascular effects from $\alpha_v\beta_3$ blockade on human endothelial cells may contribute to even greater efficacy in patients.

Although we observed that combination etaracizumab and paclitaxel *in vivo* was superior to single-agent therapy in decreasing tumor growth in the SKOV3ip1 and A2780ip2 models, such effects were not observed *in vitro*. This apparent difference between *in vitro* and *in vivo* effects may be due to an unknown function of the $\alpha_v\beta_3$ integrin within the tumor microenvironment that sensitizes tumor cells to chemotherapy and cannot be duplicated in two-dimensional culture conditions despite the presence of vitronectin. Further elucidation of such mechanisms, beyond effects on proliferation and angiogenesis, is

Table 1. Summary of Cell Line Properties and Response to Therapy.

Cell Line	$\alpha_v\beta_3$ Expression	Response to Etaracizumab	p-Akt-Dependent	Etaracizumab Increases Paclitaxel Efficacy
SKOV3ip1	High	Yes	Yes	Yes
A2780ip2	Low	No	Yes	Yes
HeyA8	High	Yes	No	No

underway and may provide additional insights into the functions of the $\alpha_v\beta_3$ integrin.

The $\alpha_v\beta_3$ integrin is an attractive target for cancer therapy. It is the primary integrin involved in angiogenesis [5]. Several preclinical studies have demonstrated effective antitumor effects in targeting $\alpha_v\beta_3$ by antibody-mediated or small molecule inhibitor approaches [11,21–24]. In addition, there is limited expression of $\alpha_v\beta_3$ on normal tissues, including minimal expression on intestinal, vascular, and uterine smooth muscle cells [36], and moderate expression on activated leukocytes, macrophages, and osteoclasts [37,38]. This favorable expression pattern is also supported by the emerging clinical experience with $\alpha_v\beta_3$ blockade. For example, in a phase I trial with etaracizumab [25], no grade 3 to 4 toxicities were noted, though most patients had grade 1 self-limited fever, chills, and malaise, a reaction commonly found with immunotherapy. One patient in this trial had ovarian cancer and had stable disease after 9 weeks of therapy. Prior studies have demonstrated a prolongation in progression-free survival in consolidation chemotherapy for ovarian carcinoma, although toxicities were significantly increased [39]. An agent that retards tumor growth with minimal adverse effects would be ideal for consolidation or maintenance therapy. Targeting $\alpha_v\beta_3$, or using similar antivascular strategies, is an attractive option in this setting.

In ovarian cancer, the α_v subunit has been found on 100% (of 30 samples) of ovarian tumors and on cells from effusions in 96% (of 121 samples) of patients [25], although the expression of the β_3 subunit was not examined. *In vitro*, migration of ovarian cancer cells has been found to be dependent on $\alpha_v\beta_3$ [11]. The $\alpha_v\beta_3$ integrin mediates adhesion to the ECM [22], and mobility of ovarian cancer cells is enhanced by $\alpha_v\beta_3$ and its interaction with vitronectin [24]. Inhibition of $\alpha_v\beta_3$ through enhanced expression of a natural ligand [40] or through the use of monoclonal antibodies has been shown to inhibit ovarian cancer cell adhesion, mobility, and migration [11,40].

There is evidence for a role of $\alpha_v\beta_3$ in multiple mechanisms of tumor growth and invasion, including interaction with ECM components, matrix metalloproteinase 2, platelet-derived growth factor, insulin, VEGF receptors, and prevention of apoptosis [33]. This is of significance not only because there may be redundant pathways to invasion and angiogenesis that can compensate for blockade of a single pathway but also because each tumor has different biologic properties and may be more dependent on one pathway than another. As we have shown, differential key processes such as $\alpha_v\beta_3$ expression and dependence on Akt may explain variable response to therapy and to combination with chemotherapy. Targeting a protein that inhibits several facets of a pathway that is common to all cancers, i.e., angiogenesis, would be a favorable method for use in all patients that may have heterogeneous tumors. However, as we have shown, even antiangiogenic therapy may have variable responses among heterogeneous tumors.

In summary, we have provided evidence for participation of the $\alpha_v\beta_3$ integrin in ovarian cancer proliferation and invasion and demonstrate that blocking the integrin with the clinically available humanized monoclonal antibody etaracizumab can inhibit tumor growth in an orthotopic mouse model of advanced ovarian cancer. Response to therapy is variable and is enhanced by dependence of the cancer cells on the Akt pathway. As development of etaracizumab continues, consideration should be given to clinical testing in ovarian cancer and, if effective, would be an attractive agent for use in recurrent cancer therapy in combination with chemotherapy. In addition,

because of its low toxicity, this antibody may also be useful in a consolidation therapy setting.

References

- [1] Hynes RO, Bader BL, and Hodivala-Dilke K (1999). Integrins in vascular development. *Braz J Med Biol Res* **32**, 501–510.
- [2] Chammas R and Brentani R (1991). Integrins and metastases: an overview. *Tumour Biol* **12**, 309–320.
- [3] Ruoslahti E (1996). Integrin signaling and matrix assembly. *Tumour Biol* **17**, 117–124.
- [4] Pytela R, Pierschbacher MD, and Ruoslahti E (1985). A 125/115-kDa cell surface receptor specific for vitronectin interacts with the arginine-glycine-aspartic acid adhesion sequence derived from fibronectin. *Proc Natl Acad Sci USA* **82**, 5766–5770.
- [5] Brooks PC, Montgomery AM, Rosenfeld M, Reisfeld RA, Hu T, Klier G, and Cheresch DA (1994). Integrin $\alpha_v\beta_3$ antagonists promote tumor regression by inducing apoptosis of angiogenic blood vessels. *Cell* **79**, 1157–1164.
- [6] Cheresch DA and Spiro RC (1987). Biosynthetic and functional properties of an Arg-Gly-Asp-directed receptor involved in human melanoma cell attachment to vitronectin, fibrinogen, and von Willebrand factor. *J Biol Chem* **262**, 17703–17711.
- [7] Charo IF, Nannizzi L, Smith JW, and Cheresch DA (1990). The vitronectin receptor $\alpha_v\beta_3$ binds fibronectin and acts in concert with $\alpha_5\beta_1$ in promoting cellular attachment and spreading on fibronectin. *J Cell Biol* **111**, 2795–2800.
- [8] Stromblad S and Cheresch DA (1996). Cell adhesion and angiogenesis. *Trends Cell Biol* **6**, 462–468.
- [9] Brooks PC (1996). Cell adhesion molecules in angiogenesis. *Cancer Metastasis Rev* **15**, 187–194.
- [10] Giancotti FG and Ruoslahti E (1999). Integrin signaling. *Science* **285**, 1028–1032.
- [11] Leroy-Dudal J, Demeilliers C, Gallet O, Pauthe E, Dutoit S, Agniel R, Gauduchon P, and Carreiras F (2005). Transmigration of human ovarian adenocarcinoma cells through endothelial extracellular matrix involves α_v integrins and the participation of MMP2. *Int J Cancer* **114**, 531–543.
- [12] Ferrara N (1995). The role of vascular endothelial growth factor in pathological angiogenesis. *Breast Cancer Res Treat* **36**, 127–137.
- [13] Folkman J (1995). Angiogenesis in cancer, vascular, rheumatoid and other disease. *Nat Med* **1**, 27–31.
- [14] Byzova TV, Goldman CK, Pampori N, Thomas KA, Bett A, Shattil SJ, and Plow EF (2000). A mechanism for modulation of cellular responses to VEGF: activation of the integrins. *Mol Cell* **6**, 851–860.
- [15] Borges E, Jan Y, and Ruoslahti E (2000). Platelet-derived growth factor receptor beta and vascular endothelial growth factor receptor 2 bind to the beta 3 integrin through its extracellular domain. *J Biol Chem* **275**, 39867–39873.
- [16] Montgomery AM, Reisfeld RA, and Cheresch DA (1994). Integrin $\alpha_v\beta_3$ rescues melanoma cells from apoptosis in three-dimensional dermal collagen. *Proc Natl Acad Sci USA* **91**, 8856–8860.
- [17] Petitclerc E, Stromblad S, von Schalscha TL, Mitjans F, Piulats J, Montgomery AM, Cheresch DA, and Brooks PC (1999). Integrin $\alpha(v)\beta_3$ promotes M21 melanoma growth in human skin by regulating tumor cell survival. *Cancer Res* **59**, 2724–2730.
- [18] Brooks PC, Stromblad S, Klemke R, Visscher D, Sarkar FH, and Cheresch DA (1995). Antiintegrin $\alpha_v\beta_3$ blocks human breast cancer growth and angiogenesis in human skin. *J Clin Invest* **96**, 1815–1822.
- [19] Lode HN, Moehler T, Xiang R, Jonczyk A, Gillies SD, Cheresch DA, and Reisfeld RA (1999). Synergy between an antiangiogenic integrin α_v antagonist and an antibody-cytokine fusion protein eradicates spontaneous tumor metastases. *Proc Natl Acad Sci USA* **96**, 1591–1596.
- [20] Gutheil JC, Campbell TN, Pierce PR, Watkins JD, Huse WD, Bodkin DJ, and Cheresch DA (2000). Targeted antiangiogenic therapy for cancer using Vitaxin: a humanized monoclonal antibody to the integrin $\alpha_v\beta_3$. *Clin Cancer Res* **6**, 3056–3061.
- [21] Markland FS, Shieh K, Zhou Q, Golubkov V, Sherwin RP, Richters V, and Sposto R (2001). A novel snake venom disintegrin that inhibits human ovarian cancer dissemination and angiogenesis in an orthotopic nude mouse model. *Haemostasis* **31**, 183–191.
- [22] Carreiras F, Thiebot B, Leroy-Dudal J, Maubant S, Breton MF, and Darbeida H (2002). Involvement of $\alpha_v\beta_3$ integrin and disruption of endothelial fibronectin network during the adhesion of the human ovarian adenocarcinoma cell

- line IGROV1 on the human umbilical vein cell extracellular matrix. *Int J Cancer* **99**, 800–808.
- [23] Maubant S, Cruet-Hennequart S, Poulain L, Carreiras F, Sichel F, Luis J, Staedel C, and Gauduchon P (2002). Altered adhesion properties and α_v integrin expression in a cisplatin-resistant human ovarian carcinoma cell line. *Int J Cancer* **97**, 186–194.
- [24] Hapke S, Kessler H, Lubber B, Bengel A, Hutzler P, Hofler H, Schmitt M, and Reuning U (2003). Ovarian cancer cell proliferation and motility is induced by engagement of integrin $\alpha_v\beta_3$ /vitronectin interaction. *Biol Chem* **384**, 1073–1083.
- [25] Davidson B, Goldberg I, Reich R, Tell L, Dong HP, Trope CG, Risberg B, and Kopolovic J (2003). α_v - and β_1 -Integrin subunits are commonly expressed in malignant effusions from ovarian carcinoma patients. *Gynecol Oncol* **90**, 248–257.
- [26] Buick RN, Pullano R, and Trent JM (1985). Comparative properties of five human ovarian adenocarcinoma cell lines. *Cancer Res* **45**, 3668–3676.
- [27] Yoneda J, Kuniyasu H, Crispens MA, Price JE, Bucana CD, and Fidler IJ (1998). Expression of angiogenesis-related genes and progression of human ovarian carcinomas in nude mice. *J Natl Cancer Inst* **90**, 447–454.
- [28] Langley RR, Ramirez KM, Tsan RZ, Van Arsdall M, Nilsson MB, and Fidler IJ (2003). Tissue-specific microvascular endothelial cell lines from H-2K(b)-tsA58 mice for studies of angiogenesis and metastasis. *Cancer Res* **63**, 2971–2976.
- [29] Gladson CL and Cheresh DA (1991). Glioblastoma expression of vitronectin and the $\alpha_v\beta_3$ integrin. Adhesion mechanism for transformed glial cells. *J Clin Invest* **88**, 1924–1932.
- [30] Felding-Habermann B, Ruggeri ZM, and Cheresh DA (1992). Distinct biological consequences of integrin $\alpha_v\beta_3$ -mediated melanoma cell adhesion to fibrinogen and its plasmic fragments. *J Biol Chem* **267**, 5070–5077.
- [31] Mitjans F, Sander D, Adan J, Sutter A, Martinez JM, Jaggle CS, Moyano JM, Kreysch HG, Piulats J, and Goodman SL (1995). An anti- α_v -integrin antibody that blocks integrin function inhibits the development of a human melanoma in nude mice. *J Cell Sci* **108** (Pt. 8), 2825–2838.
- [32] Carreiras F, Rigot V, Cruet S, Andre F, Gauduchon P, and Marvaldi J (1999). Migration properties of the human ovarian adenocarcinoma cell line IGROV1: importance of $\alpha_v\beta_3$ integrins and vitronectin. *Int J Cancer* **80**, 285–294.
- [33] Kumar CC (2003). Integrin $\alpha_v\beta_3$ as a therapeutic target for blocking tumor-induced angiogenesis. *Curr Drug Targets* **4**, 123–131.
- [34] Estep AL, Palmer C, McCormick F, and Rauen KA (2007). Mutation analysis of *BRAF*, *MEK1* and *MEK2* in 15 ovarian cancer cell lines: implications for therapy. *PLoS ONE* **2**, e1279.
- [35] COSMIC (2008). *Mutations of the A2780 Ovarian Cancer Cell Line*. [cited; Available at: <http://www.sanger.ac.uk/perl/genetics/CGP/cosmic?action=sample&id=906804>]. Accessed July 1, 2008.
- [36] Brem RB, Robbins SG, Wilson DJ, O'Rourke LM, Mixon RN, Robertson JE, Planck SR, and Rosenbaum JT (1994). Immunolocalization of integrins in the human retina. *Invest Ophthalmol Vis Sci* **35**, 3466–3474.
- [37] Ross FP, Chappel J, Alvarez JI, Sander D, Butler WT, Farach-Carson MC, Mintz KA, Robey PG, Teitelbaum SL, and Cheresh DA (1993). Interactions between the bone matrix proteins osteopontin and bone sialoprotein and the osteoclast integrin $\alpha_v\beta_3$ potentiate bone resorption. *J Biol Chem* **268**, 9901–9907.
- [38] Horton MA (1997). The $\alpha_v\beta_3$ integrin “vitronectin receptor”. *Int J Biochem Cell Biol* **29**, 721–725.
- [39] Markman M, Liu PY, Wilczynski S, Monk B, Copeland LJ, Alvarez RD, Jiang C, and Alberts D (2003). Phase III randomized trial of 12 versus 3 months of maintenance paclitaxel in patients with advanced ovarian cancer after complete response to platinum and paclitaxel-based chemotherapy: a Southwest Oncology Group and Gynecologic Oncology Group trial. *J Clin Oncol* **21**, 2460–2465.
- [40] Beck V, Herold H, Bengel A, Lubber B, Hutzler P, Tschesche H, Kessler H, Schmitt M, Geppert HG, and Reuning U (2005). ADAM15 decreases integrin $\alpha_v\beta_3$ /vitronectin-mediated ovarian cancer cell adhesion and motility in an RGD-dependent fashion. *Int J Biochem Cell Biol* **37**, 590–603.